

Ising model for melt ponds on Arctic sea ice

Yi-Ping Ma,¹ Ivan Sudakov,^{2,*} and Kenneth M. Golden²

¹*Department of Applied Mathematics, University of Colorado, Boulder, Colorado 80309, USA*

²*Department of Mathematics, University of Utah, Salt Lake City, Utah 84112, USA*

The albedo of melting Arctic sea ice, a key parameter in climate modeling, is determined by pools of water on the ice surface. Recent observations show an onset of pond complexity at a critical area of about 100 square meters. To explain this behavior and provide a statistical physics approach to sea ice modeling, we introduce a two dimensional Ising model for pond evolution which incorporates ice–albedo feedback and the underlying thermodynamics. The binary magnetic spin variables in the Ising model correspond to the presence of melt water or ice on the sea ice surface. The model exhibits a second-order phase transition from isolated to clustered melt ponds, with the evolution of pond complexity in the clustered phase consistent with the observations.

PACS numbers: 64.60.De, 92.10.Rw, 05.10.-a, 89.20.-a, 89.75.-k

Phase transitions are at heart of the very existence of the planetary cryosphere existence. Important elements of Earth’s climate system such as sea ice, permafrost, glaciers, the great land ice sheets covering Antarctica and Greenland, etc., were formed under temperature change resulting in phase transition, primarily between water and ice. Phase transitions in the cryosphere remain of continuing interest as the climate system warms, and are crucial for the stability of the climate system.

As an important example of a phase transition, during the melt season the Arctic sea ice cover becomes a complex, evolving composite of ice, melt ponds, and open water. Melting is strongly influenced by the morphological characteristics of the ice cover, such as the size and shape of melt ponds and ice floes. Albedo, light transmission, and melting are closely connected to melt pond characteristics, while floe perimeter is a primary control parameter for lateral melting. While snow and ice reflect most incident sunlight, melt ponds and ocean absorb most of it. The overall reflectance or albedo of sea ice is determined by the evolution of melt pond geometry [1, 2] and ice floe configurations [3]. As melting increases, so does solar absorption, which leads to more melting, and so on. This ice–albedo feedback has played a significant role in the decline of the summer Arctic ice pack [4], which most climate models have underestimated [5]. It is through this feedback mechanism that the phase transition between water and ice on the local scale leads to critical changes on the sea ice surface, which may be identified as a phase transition on the global scale.

A possible geometric signature of this global phase transition is found in Ref. [6], where it was discovered from analyzing images of Arctic melt ponds that the pond shape transitions from simple to complex around a critical area of 100 m². Hence in this paper we explain this phenomenon based on classical models for phase transitions such as the Ising model [7]. This approach can provide fundamental new insights into the melting process and the evolution of sea ice albedo, as well as new definitions of critical phenomena in the climate system

through classical statistical physics. See also Ref. [8] for an Ising-like model for tropical convection.

The statistical physics model proposed in this paper illustrates how an initial snow/ice topography may give rise to interconnected melt ponds over multiple years. This new model complements existing models such as Refs. [1, 9] proposed to better represent sea ice in climate models. As observed in Ref. [2], the initial ice topography that supports melt ponds results from snow melting, and so should exhibit the same spatial scale as the characteristic wavelength $l_c \approx 0.6$ m of snow piles [10]. Subsequently, melt ponds tend to drain to a constant water level guided by the preexisting ice topography and facilitated by brine channels that may connect different ponds. Since these brine channels may eventually connect melt ponds to open ocean, this water level is expected to correlate positively with the sea level. On a relatively short time scale, say for some portion of a single melting season, percolation through a fixed ice topography (see e.g. [11]) is expected to predict the melt pond pattern well. However, on a longer time scale, the ice topography changes significantly due to melting and freezing, and the percolation model by itself is no longer appropriate. Traditionally, the time evolution of the ice topography is described using partial differential equations (PDEs) that incorporate the detailed mechanisms of drainage, melting and freezing. In comparison, our new model based on statistical physics is considerably easier to formulate and implement, while retaining the essential physics.

To begin the analysis, we note that melt ponds are formed during the melting season which lasts $\tau_0 \approx 90$ days each year in the summer. In the remainder of the year, melt ponds are refrozen and so the ice topography is largely preserved until the next melting season [12]. Hence to describe the evolution of melt ponds, it suffices to account for physical processes within each melting season. The time interval for the formation of melt ponds is denoted by $t \in [0, \tau]$, namely $t = 0$ is the time before any melting occurs and $t = \tau$ is the time when melt

ponds are observed. Thus the time interval $\tau \in [0, \tau_0]$ corresponds to first-year ice, $\tau \in [\tau_0, 2\tau_0]$ corresponds to second-year ice, and so on. The key assumption of our model is that the melt pond system at time τ tends to minimize a Hamiltonian $\mathcal{H}(\tau)$ that depends on the initial ice topography denoted by h and the water level $w(t)$ where $t \in [0, \tau]$, and the height coordinate is chosen such that h has zero mean. Physically $\mathcal{H}(\tau)$ represents the thermal free energy possessed by the melt pond system at time τ . The state variable in our model is a binary variable s^i , referred to as spin in statistical physics, such that $s^i = +1$ ($s^i = -1$) corresponds to water (ice). The location index i is defined on a 2D square lattice with the lattice constant a taken to be the spatial scale l_c above. The magnetization M is defined as

$$M = \frac{1}{N} \sum_i s^i, \quad (1)$$

where N is the number of lattice sites. The pond fraction F , namely the fraction of up-spins, is therefore related to M by $M = 2F - 1$. In a pure percolation process, at any time t melt ponds drain to the water level $w(t)$ such that

$$s^i = +1 \quad (s^i = -1) \quad \text{when} \quad \eta_0^i(t) > 0 \quad (\eta_0^i(t) < 0), \quad (2)$$

where

$$\eta_0^i(t) = w(t) - h^i. \quad (3)$$

Hence at time t , for an arbitrary spin configuration s^i , we take the water depth (ice height) when $s^i = +1$ ($s^i = -1$) to be $\eta_1^i(t)$ ($\eta_2^i(t)$) where

$$\eta_1^i(t) = \max(\eta_0^i(t), 0), \quad \eta_2^i(t) = \max(-\eta_0^i(t), 0). \quad (4)$$

In the following we derive the Hamiltonian \mathcal{H} in terms of $\eta_n^i(t)$, $n = 0, 1, 2$. The physical considerations above suggest that $\mathcal{H} = \mathcal{H}_p + \mathcal{H}_m$ where \mathcal{H}_p and \mathcal{H}_m respectively represent contributions from percolation and melting.

The percolation free energy \mathcal{H}_p represents the thermal energy taken to create s^i via freezing/melting relative to the pure percolation case given by Eq. (2) with $t = \tau$. The energy released from freezing water is $L\rho_1 a^2 \eta_0^i(\tau)$, while the energy taken to melt ice is $-L\rho_2 a^2 \eta_0^i(\tau)$, where $L = 3.34 \times 10^5 \text{ J} \cdot \text{kg}^{-1}$ is the latent heat of melting, and ρ_1 (ρ_2) is the density of water (ice). To simplify the resulting expression we take $\rho \equiv \rho_1 = \rho_2 = 1 \times 10^3 \text{ kg} \cdot \text{m}^{-3}$. Hence the percolation free energy may be written as

$$\mathcal{H}_p(s^i; \tau) = -\frac{1}{2} \sum_i L\rho a^2 \eta_0^i(\tau) s^i. \quad (5)$$

The melting free energy \mathcal{H}_m represents the thermal energy transferred between neighboring sites in the entire melting process $t \in [0, \tau]$. Assuming for simplicity that the water temperature $\Theta_w > 0$ is independent of

location and time and the ice temperature is identically zero (both measured in Celsius), the energy transferred between either two water sites or two ice sites is then identically zero. Between a water site i and an ice site j , the heat flux is $\phi_1 = \kappa_1 \nabla \Theta$ ($\phi_2 = \kappa_2 \nabla \Theta$) on the water (ice) side, where $\nabla \Theta = \Theta_w/a$, and $\kappa_1 = 1.4 \times 10^{-7} \text{ m}^2 \text{ s}^{-1}$ ($\kappa_2 = 1.3 \times 10^{-6} \text{ m}^2 \text{ s}^{-1}$) is the thermal diffusivity of water (ice). The energy transfer rate at time t is therefore respectively given by $\phi_1 k_1 \rho a \eta_1^i(t)$ for the energy released by the water site, and $\phi_2 k_2 \rho a \eta_2^j(t)$ for the energy received by the ice site, where $k_1 = 4.2 \times 10^3 \text{ J} \cdot \text{kg}^{-1} \text{ deg}^{-1}$ ($k_2 = 2.1 \times 10^3 \text{ J} \cdot \text{kg}^{-1} \text{ deg}^{-1}$) is the specific heat of water (ice). Hence the melting free energy takes the form

$$\mathcal{H}_m(s^i; \tau) = \sum_{\substack{\langle i, j \rangle: \\ s^i > 0, s^j < 0}} \rho \tau_0 \Theta_w \times \left(\kappa_1 k_1 \alpha_1^i(\tau) + \kappa_2 k_2 \alpha_2^j(\tau) \right), \quad (6)$$

where $\langle i, j \rangle$ denote nearest neighbor pairs, and

$$\alpha_n^i(\tau) = \frac{1}{\tau_0} \int_0^\tau \eta_n^i(t) dt, \quad n = 1, 2. \quad (7)$$

Therefore the total free energy is, after normalization

$$\mathcal{H}(s^i; \tau) = - \sum_i \eta_0^i(\tau) s^i + \sum_{\substack{\langle i, j \rangle: \\ s^i > 0, s^j < 0}} \left(J_1 \alpha_1^i(\tau) + J_2 \alpha_2^j(\tau) \right), \quad (8)$$

where $J_n = 2k_n \kappa_n \tau_0 \Theta_w / (La^2)$, $n = 1, 2$. Now the only physical parameter to be specified is the water temperature Θ_w . Since water has lower albedo than ice, larger pond fraction F leads to more absorbed solar radiation and thus higher Θ_w . For simplicity we take $\Theta_w = 8F$ based on the observation that $\Theta_w = 2$ when $F = 25\%$ [12, 13]. Hence in terms of the magnetization M we have

$$J_n = \mathcal{J}_n(M + 1), \quad n = 1, 2, \quad (9)$$

where $\mathcal{J}_1 = 0.3$ and $\mathcal{J}_2 = 5\mathcal{J}_1$. The statistical physical model defined by Eqs. (8-9) will be referred to as the percolation-melting Ising model (PMIM).

The PMIM is similar to the classical random field Ising model (RFIM) (see e. g. [14]) due to the presence of a random external magnetic field and ferromagnetic coupling between neighboring spins. However, in the PMIM the coupling constant is nonzero only between antiparallel spins, and depends on both the local external magnetic fields and the overall magnetization. The latter dependence implies that as the overall magnetization increases, the coupling constants also increase, which leads to more clustering of parallel spins and therefore even higher overall magnetization. This analog of ice-albedo feedback is essential for the novel properties of the PMIM, including in particular a new phase transition as detailed below.

In the following we present Monte Carlo (MC) simulation results for the PMIM at temperature T . For $T \approx 0$

we use 10 MC steps since the system is expected to converge rapidly to a minimum of \mathcal{H} . For larger T we use up to 100 MC steps to reach statistical equilibrium. Unless otherwise stated, the number of lattice sites N is taken to be 1024×1024 . For simplicity we choose h^i to be independent Gaussian variables with zero mean and unit variance, and $w(t)$ to be the following sinusoid

$$w(t) = w_0 + w_1 \cos(2\pi t/\tau_0), \quad (10)$$

where the period is taken to be the duration of the melting season $\tau_0 = 90$ days. Unless otherwise stated, the coefficients in Eq. (10) are chosen to be $w_0 = -0.1$ and $w_1 = -0.5$, such that the pond fraction varies between 10% and 40% consistent with observations [2], or equivalently the magnetization varies between -0.8 and -0.2 as shown in Fig. 1(a). A more realistic expression for $w(t)$ may be deduced from ODE models for sea ice (see e.g. Ref. [9]).

Figure 1 shows the MC simulation results at a very low temperature $T = 0.01$. Figure 1(a) shows the magnetization M as a function of time τ ; the spin configurations s^i at the labeled points (i)–(iv) are shown right below. Comparing panel (i)/(iii) with (ii)/(iv), we see that within a single period, $M(\tau)$ varies in accordance with $w(\tau)$ with maxima (minima) attained in the middle (end) of the period. For $\tau > 0$, $M(\tau)$ is always lower than the magnetization $M_p(\tau)$ computed for pure percolation, namely at $\mathcal{J}_1 = \mathcal{J}_2 = 0$. Over multiple periods, $M(\tau)$ gradually decreases towards $M = -1$, consistent with observations on multi-year ice in Ref. [15].

The spin configurations in Fig. 1(i)–(iv) may be classified into an isolated phase and a clustered phase, where the ponds are respectively isolated (panels (ii) and (iv)) and clustered (panels (i) and (iii)). The existence intervals of these two phases can be readily identified from the plot of the first derivative $M'(\tau)$ as shown in Fig. 1(b). For $\tau \in [0, \tau_1^+]$, $M'(\tau)$ is smooth and the system remains in the isolated phase. At $\tau = \tau_1^+$, $M'(\tau)$ increases discontinuously and the system transitions from the isolated phase to the clustered phase. For $\tau \in [\tau_1^+, \tau_1^-]$, $M'(\tau)$ is smooth and the system remains in the clustered phase. At $\tau = \tau_1^-$, $M'(\tau)$ increases discontinuously again and the system transitions from the clustered phase back to the isolated phase. These processes are then repeated in the following periods, while the existence interval of the clustered phase $\tau \in [\tau_k^+, \tau_k^-]$ shrinks as k increases. Thus after sufficiently many periods, it is expected that the clustered phase vanishes and the isolated phase persists. The transition between these two phases is identified as second-order due to the discontinuity in the first derivative of the order parameter M .

The effect of external noise on melt pond evolution, resulting for example from atmospheric forcing [17], can be studied using the PMIM at finite temperature T . Figure 2(a) shows the MC simulation results at the same parameters as in Fig. 1(iii) but for varying T . It can be seen

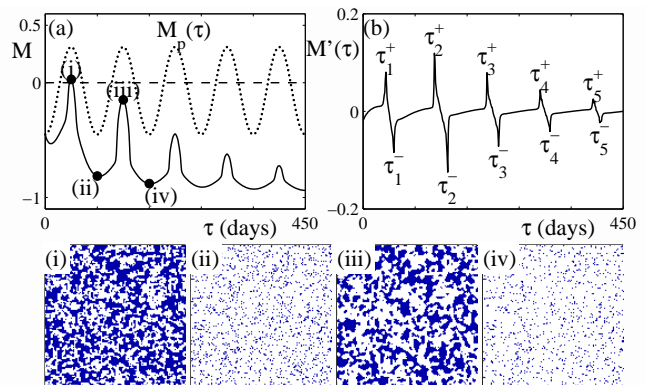


FIG. 1. MC simulation results for the PMIM defined by Eq. (8–9) at $T = 0.01$. (a) Plot of the magnetization M as a function of time τ . The period $\tau_0 = 90$ days represents the duration of the melting season; thus the time interval $[(k-1)\tau_0, k\tau_0]$ corresponds to k -th year ice. The function $M_p(\tau)$ represents $M(\tau)$ computed at $\mathcal{J}_1 = \mathcal{J}_2 = 0$. The spin configurations s^i at the labeled points are shown on a 128×128 domain with (i) $\tau = 45$; (ii) $\tau = 90$; (iii) $\tau = 135$; (iv) $\tau = 180$. The up-spins and down-spins are respectively shown in blue and white. See [16] for an animation of panels (i–iv). (b) Plot of the first derivative $M'(\tau)$. The value of τ at the maximum (minimum) of $M'(\tau)$ in the k -th period is denoted by τ_k^+ (τ_k^-).

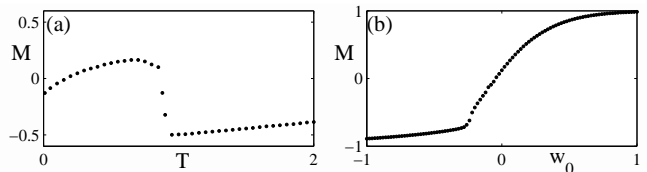


FIG. 2. The magnetization M of the PMIM at the same parameters as in Fig. 1(iii) but for varying temperature T (panel (a)) or mean water level w_0 (panel (b)).

that as T increases, the magnetization M first increases slowly, then decreases sharply at a critical temperature $T_c \approx 0.9$, and increases slowly again. At $T = T_c$, the system appears to transition from the clustered phase to the isolated phase. Assuming that the external noise is small [17], then only the low temperature regime $T < T_c$ is physically relevant.

The effect of climate change on melt pond evolution can also be studied using the PMIM in the low temperature regime. The main sea ice parameter that responds to climate change is the overall thickness of the ice pack. This in turn affects melt ponds through the mean water level w_0 , which decreases as the ice pack thickens and vice versa. Figure 2(b) shows the PMIM at the same parameters as in Fig. 1(iii) but for varying w_0 . As w_0 increases the system transitions from the isolated phase to the clustered phase at $w_0 \approx -0.24$.

The up-spin clusters in Fig. 1(iii) at $\tau = 1.5\tau_0$ correspond to well developed melt ponds on multi-year ice

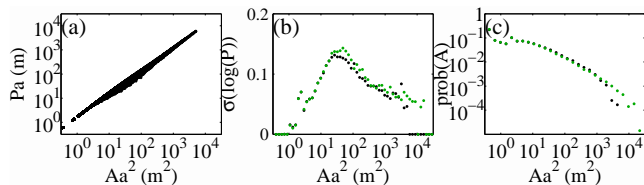


FIG. 3. Area perimeter plots for the up-spin clusters in Fig. 1(iii) at $T = 0.01$ and $T = 0.05$. (a) Log-log plot of the perimeter P versus the area A at $T = 0.01$. (b) Plot of the variance $\sigma(\log(P))$ as a function of A (log scale). (c) Log-log plot of the probability $\text{prob}(A)$ as a function of A . For (b-c), the $T = 0.01$ and $T = 0.05$ cases are respectively shown in black and green. To compare with observations, A and P are shown in physical units with the lattice constant $a = 0.6$ m. The number of lattice sites N is increased to 4096×4096 to improve the statistics.

or transition zones in Ref. [6]. Indeed in this case, the shapes of the smaller clusters are relatively simple while those of the larger clusters are more complex. We remark that the coexistence of spin clusters has also been observed in the classical RFIM [18]. To facilitate comparison with observations in Ref. [6], the area A and the perimeter P in the PMIM are shown in physical units as Aa^2 and Pa where appropriate, with $a = 0.6$ m being the lattice constant as stated above.

Figure 3(a) shows the log-log plot of P versus A for these clusters at $T = 0.01$. It can be seen that similar to Ref. [6], the lower edge of the cluster of points exhibits a change of slope at a critical area A_c . To quantify the onset of complexity, we define the elasticity as the variance σ of $\log(P)$, and identify the onset of complexity with maximum elasticity. Fig. 3(b) shows the elasticity $\sigma(\log(P))$ as a function of A for $T = 0.01$ (black dots) and $T = 0.05$ (green dots). It can be seen that there indeed exists a critical area A_c , such that $\sigma(\log(P))$ increases (decreases) approximately linearly with $\log(A)$ for simple (complex) ponds with $A < A_c$ ($A > A_c$). As T increases, the critical area A_c increases slightly, while the elasticity $\sigma(\log(P))$ remains almost unchanged for simple ponds but increases slightly for complex ponds. The maximum elasticity occurs at a critical area of $A_c a^2 \approx 50$ m^2 , which agrees well with the observed critical area of about 100 m^2 in Ref. [6].

To compare with recent mapping of melt ponds in Ref. [15], Fig. 3(c) shows the log-log plot of the probability distribution $\text{prob}(A)$ as a function of the area A for $T = 0.01$ (black dots) and $T = 0.05$ (green dots). It can be seen that the probability exhibits a power law scaling as a function of area, which agrees with the observations made in Ref. [15]. As T increases, the probability remains almost unchanged except that the power law scaling extends to even larger area.

Finally, we remark that the above transition between the isolated and clustered phases in the PMIM is also

found in the following simplified model

$$\mathcal{H}(s^i) = - \sum_i (w - h^i) s^i - J(M + 1) \sum_{\langle i,j \rangle} s^i s^j, \quad (11)$$

where w and $J > 0$ are constants. This model differs from the classical RFIM only in that the coupling constant increases with the overall magnetization, and thus may be of considerable theoretical interest.

In this paper we have proposed a two-dimensional Ising model, referred to as the percolation-melting Ising model (PMIM), to describe the evolution of Arctic melt ponds. As long as the external noise is small, the system always evolves into an ordered phase where the ponds are either isolated (the isolated phase) or clustered (the clustered phase). The clustered phase is present for part of the melting season and features coexistence between simple and complex ponds. The critical area for the onset of complexity is found to be consistent with the observations made in Ref. [6]. The transition between the isolated and clustered phases is found to be second-order. This phase transition may be interpreted as a tipping mechanism in sea ice-albedo feedback [9]. The detailed understanding of Arctic melt ponds pursued in this paper may advance our ability to model the future trajectory of the Arctic sea ice pack (e.g., through parameterizing Global Climate Models [19]).

The statistical physical approach developed in this paper may be generalizable to closely related systems such as Arctic permafrost lakes [20].

We gratefully acknowledge support from the Division of Mathematical Sciences and the Division of Polar Programs at the U.S. National Science Foundation (NSF) through Grants DMS-1009704, ARC-0934721, DMS-0940249, and DMS-0940262. We are also grateful for support from the Office of Naval Research (ONR) through Grant N00014-13-10291. Finally, we would like to thank the NSF Math Climate Research Network (MCRN) for their support of this work.

* Corresponding author.
sudakov@math.utah.edu

- [1] F. Scott and D.L. Feltham, *J. Geophys. Res. Oceans* **115**, C12064 (2010).
- [2] C. Polashenski, D. Perovich, and Z. Courville, *J. Geophys. Res. Oceans* **117**, C01001 (2012).
- [3] T. Toyota, S. Takatsuji, and M. Nakayama, *Geophys. Res. Lett.* **33**, L02616 (2006).
- [4] D.K. Perovich, J.A. Richter-Menge, K.F. Jones, and B. Light, *Geophys. Res. Lett.* **35**, L11501 (2008).
- [5] M.C. Serreze, M.M. Holland, and J. Stroeve, *Science* **315**, 1533 (2007).
- [6] C. Hohenegger, B. Alali, K.R. Steffen, D.K. Perovich, and K.M. Golden, *Cryosphere* **6**, 1157 (2012).

- [7] J.M. Yeomans, *Statistical Mechanics of Phase transitions* (Oxford University Press, Oxford, 1992).
- [8] A.J. Majda and B. Khouider, Proc. Natl. Acad. Sci. U.S.A. **99**, 1123 (2002).
- [9] I. Eisenman and J.S. Wettlaufer, Proc. Natl. Acad. Sci. U.S.A. **106**, 28 (2009).
- [10] K.A. Mitchell and T. Tiedje, J. Geophys. Res. Earth Surf. **115**, F04039 (2010).
- [11] M.B. Isichenko, Rev. Mod. Phys. **64**, 961 (1992).
- [12] D. Schroeder, D.L. Feltham, D. Flocco, and M. Tsamados, Nat. Clim. Chang. **4**, 353 (2014).
- [13] P.V. Bogorodskii, A.V. Marchenko, and A.V. Pnyushkov, Oceanology **47**, 636 (2007).
- [14] T. Nattermann, *Theory of the Random Field Ising Model*, in *Spin Glasses and Random Fields*, edited by A. P. Young (World Scientific, Singapore, 1998), p. 277.
- [15] D-J. Kim, P. Hwang, K.H. Chung, S.H. Lee, H-S. Jung, and W.M. Moon, Proc. IEEE **101**, 748 (2013).
- [16] See [URL will be inserted by publisher] for the accompanying movie.
- [17] W. Moon, and J.S. Wettlaufer, J. Math. Phys. **54**, 123303 (2013).
- [18] A. Moreo, M. Mayr, A. Feiguin, S. Yunoki, and E. Dagotto, Phys. Rev. Lett. **84**, 5568 (2000).
- [19] D. Flocco, D.L. Feltham, and A.K. Turner, J. Geophys. Res. Oceans **115**, C08012 (2010).
- [20] I. Sudakov and S.A. Vakulenko, IMA J. Appl. Math. **10**, 1093 (2014).